GEOPHYSICS

Seismically determined elastic parameters for Earth's outer core

Jessica C. E. Irving[1]*, Sanne Cottaar[2], Vedran Lekić[3]

Turbulent convection of the liquid iron alloy outer core generates Earth's magnetic field and supplies heat to the mantle. The exact composition of the iron alloy is fundamentally linked to the processes powering the convection and can be constrained by its seismic properties. Discrepancies between seismic models determined using body waves and normal modes show that these properties are not yet fully agreed upon. In addition, technical challenges in experimentally measuring the equation-of-state (EoS) parameters of liquid iron alloys at high pressures and temperatures further complicate compositional inferences. We directly infer EoS parameters describing Earth's outer core from normal mode center frequency observations and present the resulting Elastic Parameters of the Outer Core (EPOC) seismic model. Unlike alternative seismic models, ours requires only three parameters and guarantees physically realistic behavior with increasing pressure for a well-mixed homogeneous material along an isentrope, consistent with the outer core's condition. We show that EPOC predicts available normal mode frequencies better than the Preliminary Reference Earth Model (PREM) while also being more consistent with body wave–derived models, eliminating a long-standing discrepancy. The velocity at the top of the outer core is lower, and increases with depth more steeply, in EPOC than in PREM, while the density in EPOC is higher than that in PREM across the outer core. The steeper profiles and higher density imply that the outer core comprises a lighter but more compressible alloy than that inferred for PREM. Furthermore, EPOC's steeper velocity gradient explains differential SmKS body wave travel times better than previous one-dimensional global models, without requiring an anomalously slow ~90- to 450-km-thick layer at the top of the outer core.

INTRODUCTION

Identified as a liquid region deep in Earth nearly a century ago (*1*), the outer core is composed of a liquid iron alloy (*2*), which convects vigorously, sustaining the geodynamo and providing heat to the mantle. The vigorous convection implies that, away from boundaries, the outer core should be well mixed and that physical properties should vary with depth along an adiabat (*3*); lateral variations are expected to be very small. To accurately characterize the elastic properties of the outer core, seismologists have produced different models for the outer core based mainly on normal mode (*4*–*6*) or body wave (*7*, *8*) measurements. Body waves alone cannot constrain variations in density, while normal modes have less sensitivity to gradients of the physical properties (*9*). These seismological models are parameterized in a variety of different ways: from smooth functions, such as polynomials, to layered or point-wise depictions. The parameterizations are chosen for convenience but can lead to unphysical models (*10*). Moreover, they do not exploit the complementary information provided by an understanding of material behavior under high pressure. It is therefore prudent to appeal to physics to further constrain models of the material properties of the outer core. Equations-of-state (EoSs) used by mineral physicists are the optimal way to represent the physical properties and behavior of a well-mixed isochemical material under pressure. Here, we invert seismic data directly for EoS parameters; this leads to the first mineral physically self-consistent model of the outer core elastic structure.

To date, the Preliminary Reference Earth Model (PREM) (*6*) is the most commonly used model for constraining the composition of the outer core (*11*–*13*). Produced in response to the scientific community's need for "a standard model for the structure of the Earth," PREM was constructed to fit the mass and moment of inertia of Earth, center frequencies and attenuation of normal modes, and travel times of body waves. Sensitivity to outer core structure was provided by body wave phases SKS and PKP, and a subset of outer core–sensitive normal modes. PREM was created using a least-squares inversion with a starting model that obeyed the Adams-Williamson equation in the outer core. The outer core of PREM is close to adiabatic and homogeneous, with the Bullen parameter, η, close to 1 throughout. PREM describes the outer core in terms of two third-order polynomials, one depicting compressional velocity (v_P) and the other depicting density (ρ). While not based on the physical properties of the material or region, and implying unphysical limiting behavior (*10*), this conservative parameterization is straightforward to implement. Two previous analyses using normal mode data (*14*, *15*) have assessed possible density deviations from PREM; however, neither work assesses velocity and density simultaneously.

Most recent models of Earth structure describe velocity alone, rather than together with density. They are derived using a variety of different body wave phases and described using several different parameterizations (*7*, *8*, *16*). Discrepancies exist between the velocities in these models and PREM. At the core-mantle boundary (CMB), PREM has a velocity greater than that in both SP6 and ak135 models, by 0.11 and 0.06 km/s, respectively. Velocities are more comparable in the mid-outer core but diverge near the inner core boundary (ICB). Observations of SmKS body wave phases have been used to advocate for the presence at the top of the outer core of a layer anomalously slow compared to PREM, which ranges in thickness from 90 km (*17*) to 300 km (*18*, *19*) and even 450 km (*20*).

Here, we reassess the elastic properties of the outer core using a physically consistent parameterization and an expanded data set of spheroidal mode center frequencies, many of which were measured on spectra from multiple great earthquakes that have occurred in the past two decades. We are, in essence, fitting the elastic parameters of an "uncertain mixture of all the elements" and using mineral physics to overcome the

[1]Department of Geosciences, Princeton University, Princeton, NJ 08540, USA. [2]Department of Earth Sciences, University of Cambridge, Cambridge, UK. [3]Department of Geology, University of Maryland, College Park, MD 20742, USA.
*Corresponding author. Email: jirving@princeton.edu

"vague suggestion" or "trivial objection" that there are too many unknown variables to fully understand the outer core's properties [see (*2*)]. We discuss the implications of our new model for the composition and dynamics of the outer core and the potential of a stratified compositionally anomalous layer at the top of the outer core.

RESULTS

Elastic parameters for the outer core

We exploit the dependence of normal mode center frequencies on the one-dimensional (1D) structure of Earth and their relative insensitivity to asphericity, rotation, and lateral heterogeneity to investigate plausible ranges for elastic parameters, which describe the seismic velocity and density of the outer core. Our mode data set contains 319 center frequency measurements assembled from a range of previously published sources (*21*–*25*). It includes 79 individual modes that were not used when PREM was constructed and is based on more recent observations, using more seismic data, than had been previously available. More than a third (22 of 64) of modes that are substantially sensitive to the outer core (more than 10% of their sensitivity) were not present in the PREM data set. The center frequency measurements are corrected for the first-order effects of Earth's ellipticity (*26*).

Because we confine our inversion to the outer core, we must assume that PREM represents the 1D structure outside it. This assumption introduces additional uncertainty into our inferences about outer core structure. To partially account for this added uncertainty, we set the measurement uncertainty for each mode so that it is the larger of the change in frequency produced by swapping two 1D reference models [PREM and STW105 of (*27*)] or the average of the change for all modes used.

The seismic properties of the outer core are found by directly seeking the parameters of an isentropic Vinet EoS (*28*) or Birch-Murnaghan EoS (*29*). Both EoSs are expressed by the bulk modulus at ambient conditions (K_{0S}), the derivative of the bulk modulus with pressure (K'_{0S}), the molar mass (M), and the molar volume at ambient conditions (V_0). As our data are only sensitive to molar density $\rho_0 \left(= \frac{M}{V_0} \right)$, the parameters M and V_0 would perfectly trade off in an inversion. To avoid this, we fix M at 0.05 kg/mol (~10% less than pure iron). The BurnMan software (*30*) is used to convert these parameters to v_p and ρ profiles across the outer core, iterating the computation to obtain self-consistent pressures (*31*).

Parameter values and uncertainties are obtained within a Bayesian framework by a Markov chain Monte Carlo search of the model space, using the Adaptive Metropolis method as implemented in PyMC (*32*). Simple prior tests assign low likelihoods to wildly unrealistic models to avoid computing the center frequencies for these models and speed up convergence (see section S5). For each proposed model that passes our prior tests, we compute normal mode eigenfrequencies using Mineos (*33*, *34*), thereby accounting for their nonlinear dependence on model parameters (see section S7). The likelihood of a proposed model being accepted is based on the sum of the log likelihoods of the predicted frequencies, assuming a Gaussian distribution around each center frequency with a standard deviation (SD) equal to the assigned mode uncertainty. The parameters are jointly updated using an adaptive stepping method, which is fine-tuned during the run by the covariance matrix of parameters in previously accepted models. Following a burn-in period and after thinning, accepted models yield an ensemble solution, which can be analyzed to quantify most likely parameter values, as well as associated uncertainties and trade-offs, as shown in Fig. 1.

Parameterizing with an EoS has the implicit advantage that the resulting model is guaranteed to correspond to a well-mixed homogeneous material, that is, the Bullen parameter ~ 1 and the Brunt-Väisälä frequency ~ 0, in agreement with our understanding of the nature of the outer core. The parameterization is well suited for the outer core but is not readily extendable to the rest of Earth, where the 1D structure is expected to deviate from isentropic EoSs due to the presence of 3D heterogeneity, phase transitions, anisotropy, spin transitions, and broad boundary layers.

Velocity and density models

The ensemble of Vinet EoS parameters for the model (Fig. 1) can be used to compute the corresponding velocity and density models (Fig. 2). While the range of values that the EoS parameters span is wide, the resulting density and especially velocity models exhibit much narrower distributions. The velocity and density models are more variable close to the ICB, where the modes in our data set have reduced sensitivity. The velocity and density models obtained from the ensemble of Birch-Murnaghan EoS parameters are very close to the Vinet-derived ones ($|\Delta v_p| < 0.02$ km/s and $|\Delta\rho| \leq 0.001$ g/cm^3), but the different extrapolations from core to ambient conditions result in different values of the EoS parameters (see section S2).

The values of EoS parameters in the ensemble solution appear to correlate strongly, indicating that there are substantial trade-offs between acceptable values of each parameter, although the trade-offs do not necessarily follow a linear relationship. It is therefore clear that the variations of each parameter (Table 1) should not be considered independently. We summarize the parameter distributions using the median parameter value and ranges containing two-thirds of the parameters, by analogy to the 1σ range of normally distributed values. Our EoS parameters are isentropic ones; they should not be compared directly to those derived from isothermal calculations or measurements. For the purpose of comparison with other studies, the parameters can be converted to isothermal parameters by choosing both a geotherm for the outer core and appropriate thermal parameters. Our parameters can also be converted to those for a different molar mass value such as an experimentally determined one, by refitting the velocities and densities in the outer core to an EoS assuming the desired molar mass. The parameters can, however, be directly used to extrapolate other planetary cores, assuming a similar composition and state to Earth's core.

The final velocity and density models for Elastic Parameters of the Outer Core–Vinet (EPOC–Vinet) are produced by combining the median Vinet EoS mineral physics parameters. Alternatively, we could use each set of mineral physics parameters in the ensemble to generate velocity and density models and then calculate the median (or 50th centile) of all the velocity models and the median of all the density models. Relative to these 50th centile models, the EPOC–Vinet model has velocities within 0.0003 km/s and densities within 0.01 g/cm^3 across the outer core, so combining the EoS parameters in this way represents the average velocity and density models well.

The EPOC model reduces the overall reduced χ^2 misfit from 1.54 for PREM to 1.02 156 (33.9% reduction), and from 2.51 to 0.74 (70.5% reduction) for the modes that have more than 10% of their integrated sensitivity in the outer core. EPOC is therefore much more representative of the true properties of the outer core than is PREM.

To facilitate physical comparison between EPOC and PREM, we compute the best-fit parameters of our Vinet EoS to the velocity and density of PREM. PREM velocity and density are fit by the EoS to less than 0.1% deviation across most of the outer core and to 0.2% near the

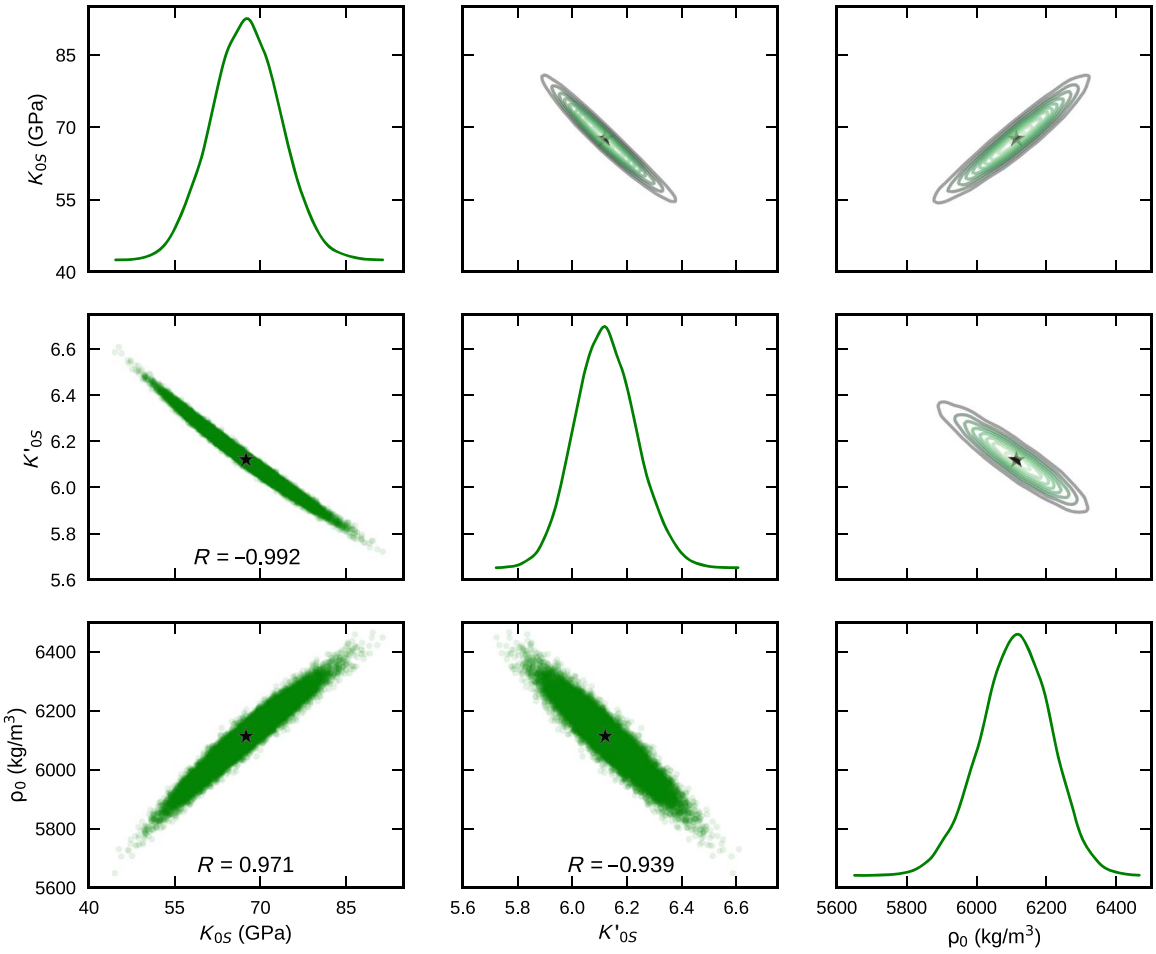

Fig. 1. Vinet EoS parameter posterior distributions and trade-offs. ρ_0 is presented using the fixed molar mass of 0.05 kg and inverted molar volume. The black stars show the median values used for the EPOC-Vinet model in Fig. 2. Numbers on the lower left panels indicate correlation coefficients between the parameters in question.

ICB. Comparison of the EoS parameters for EPOC and PREM is shown in Table 1. The value for molar density that fits PREM falls at the high end of the bounds encompassing two-thirds of molar density values for EPOC, while the PREM value for K_{0S} falls above the bounds for EPOC, and the PREM value for K'_{0S} falls below the bounds for EPOC. The PREM values are always within the model space volume sampled in our ensemble. The differences between the PREM and EPOC EoS parameters imply that the profiles for EPOC would be interpreted as a different iron alloy than those for PREM.

Differences between EPOC and PREM EoS parameters can result from differences in the inversion methodology or differences in the data used for the inversion. We assessed the effect of our methodology by inverting the data used in the PREM paper corresponding to the 240 modes present in both studies (the "PREM data"). We found that when the PREM data are used, the velocities near the CMB are similar to those in PREM, while the density and velocity in the lower outer core are different from those in PREM (section S3). Thus, we conclude that the combined effect of our Bayesian modeling approach and the new data set is responsible for the differences between EPOC-Vinet and PREM.

To assess how our model would change if a different Earth model was assumed outside of the outer core, we repeated our inversion using a version of STW105 elsewhere for Earth instead of PREM (section S4). We find that velocities change by 0.033 km/s or less everywhere in the outer core, with the velocity at the CMB becoming even lower than that in EPOC-Vinet. Using STW105 instead of PREM outside the core resulted in higher densities everywhere in the outer core than those found in both EPOC-Vinet and PREM. Based on this test, we conclude that the assumption of 1D structure outside the outer core does not affect the main conclusions of this paper.

DISCUSSION

Comparison to body wave models

Body wave models of the outer core prescribe velocities that are lower than PREM at the CMB—by 0.06 km/s for ak135 (*7*) and by 0.11 km/s for SP6 (*8*). The outer core of iasp91 (*35*) is that of the older mode and body wave–based model Parametric Earth Model (PEM) (*5*); this also has a velocity 0.06 km/s lower than PREM. Our EPOC-Vinet model has a velocity of 8.00 km/s at the CMB; this is also lower than PREM and similar to the CMB velocities of ak135 and iasp91. Calculations of a range of differential travel times (see section S6) reveal that the EPOC-Vinet model predicts outer core phase differential travel times that are often closer to the body wave models than PREM. Thus, EPOC appears to naturally reconcile normal mode and body wave models in a physically realistic parameterization even without jointly inverting

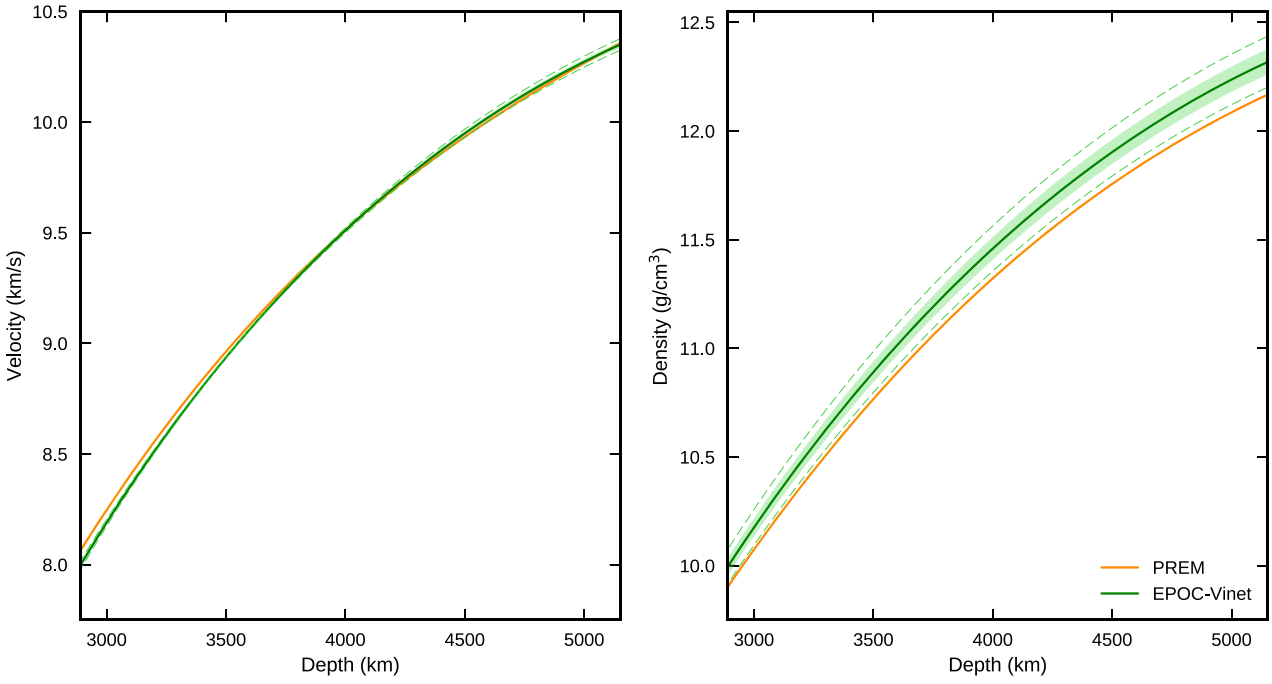

Fig. 2. The EPOC-Vinet velocity and density models. *P* wave or bulk sound velocities (**left**) and densities (**right**) for EPOC-Vinet (green) compared to PREM (orange lines). The models produced by the median parameters are shown as the dark green lines, the shaded region encompasses two-thirds of the values, and the dashed lines encompass 95% of the values at each depth.

Table 1. Elastic parameters for the outer core for EPOC-Vinet and for a Vinet EoS fit to PREM. Molar mass is fixed in the inversion at 0.05 kg. The values in brackets encompass two-thirds of the parameter values.

	EPOC-Vinet	PREM-Vinet
K_{0S} (GPa) Reference isentropic bulk modulus	67.5 (61.7–73.3)	79.7 —
K'_{0S} Pressure derivative of K_{0S}	6.12 (6.02–6.23)	5.89 —
ρ_0 (kg/m^3) Reference molar density	6110 (6010–6210)	6210
V_0 (m^{-3}) Reference molar volume	8.18×10^{-6} (8.05×10^{-6}–8.32×10^{-6})	8.06×10^{-6}

the two data types. At the ICB, the range of velocities described by the accepted EoS models widens as a result of declining sensitivity of normal modes toward the base of the outer core.

The uppermost outer core

A number of seismic body wave and geodynamical studies have suggested that the top of the outer core may exhibit a compositionally [or thermally (*36*)] anomalous stratified layer. A seismically slow layer is suggested with layer thicknesses ranging from 90 to 450 km (*17*–*20*). Observations of geomagnetic fluctuations are consistent with waves that are excited in a 140-km-thick stratified layer (*37*). A compositionally stratified layer could be enriched in light elements with potential causes including light elements excluded from inner core growth accumulating at the top of the outer core (*38*, *39*), dissolution of mantle material (*40*, *41*), relics of planetary core formation (*42*), or remnants of the moon-forming impact (*42*, *43*). In general, models of this layer's formation predict a thickness of 100 km or less (*38*–*40*). Beyond the uncertainty in the thickness of the layer, a concern remains that enrichment in any single light element would produce a seismically fast, rather than slow, layer (*44*). Furthermore, the presence of more than one light element may cause light compounds such as SiO or MgO (*45*–*47*) to form, again leading to a seismically fast layer.

The seismic evidence for an anomalously slow layer atop the outer core is based on differential travel times between SmKS phases [where m ranges between 2 and 5 and refers to the phase with (m − 1) underside reflections at the CMB]. Typically, the differential times are compared with predictions from PREM (*17*–*20*). EPOC suggests that, over a broad depth range, the uppermost outer core is slower than PREM, with a velocity difference of more than 0.06 km/s at the CMB. Figure 3 shows differential SmKS times predicted for EPOC in comparison to the published observations of Helffrich and Kaneshima (*18*), as well as predictions made using PREM, ak135, SP6, and iasp91. EPOC, which is purely based on normal modes, does a better job than other global 1D models at explaining these SmKS differential travel time observations, especially for S3KS-S2KS times at shorter distances.

While, in line with predictions from some geodynamical and geomagnetic studies, a thin compositionally or thermally anomalous layer may exist, using our updated reference model reduces the need for a thick, anomalously slow velocity layer at the top of the outer core. We therefore emphasize that the choice of background model is of paramount importance when interpreting SmKS observations.

Implications for the outer core composition and dynamics

The Bullen parameter (Eq. 1) has long been used to determine whether a region is homogeneous and adiabatic ($\eta = 1$) or instead contains phase changes ($\eta > 1$) or thermal boundary layers ($\eta < 1$)

$$\eta = \frac{d\kappa}{dP} + \frac{1}{g}\frac{d}{dr}\left(\frac{\kappa}{\rho}\right) \quad (1)$$

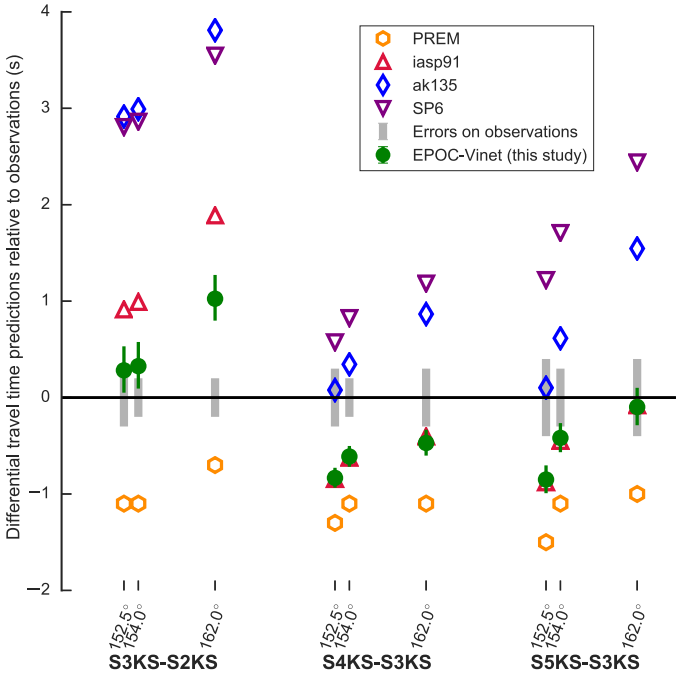

Fig. 3. SmKS differential travel time predictions. Predictions made for EPOC-Vinet, PREM, ak135, iasp91, and SP6 (*60*) are compared to body wave array-based observations from three events and for three phase pairs from (*18*). The green error bars represent predictions using the velocity ranges in table S3.

PREM's deviations from ($\eta = 1$) in the outer core are considered to be insignificant (*26*), but for EPOC, η is much closer to 1 due to our parameterization, which describes a well-mixed outer core.

The Brunt-Väisälä frequency [N; which can be written in terms of the Bullen parameter, where $N^2 = \rho g^2 (\eta - 1)/\kappa$)] determines whether a parcel of fluid moved away from its equilibrium position starts oscillating at frequency N ($N^2 > 0$), is gravitationally stable ($N^2 = 0$), or accelerates, indicating an unstable stratification ($N^2 < 0$). EPOC predicts models with squared Brunt-Väisälä frequencies close to zero throughout the outer core, indicating an outer core that is close to neutral stability. Our parameterization cannot represent thin layers of the outer core, which may correspond to stably stratified regions at either the innermost or outermost boundaries of the outer core, and the sensitivity of our data set to these deviations needs to be further tested.

The outer core's composition is often assessed by noting how changes in velocity as a function of density in the outer core compare with the results of mineral physics experiments or computations; linear behavior is consistent with Birch's law (*48*, *49*). Figure 4 shows that, while the gradients of PREM and EPOC are similar, there is a systematic offset between the two models so that EPOC has a higher density than PREM at any given velocity. The relationship between v_P and ρ can be compared directly with the results of other isentropic EoSs for various materials or for isothermal EoSs to which temperature corrections have been applied.

In both the mineral physics parameterizations, the density of the outer core is less tightly constrained than its velocity. Most of the reduction of the χ^2 misfit is due to the updated velocity profile as opposed to the updated density profile. The density of the EPOC models is greater than that of PREM, with EPOC-Vinet showing an increase of 0.94 to 1.25% across the core. This yields a core that is more massive (0.35% of $M_\oplus$) and contains more moment of inertia (0.13% of $I_\oplus$) than the PREM core. For the sake of comparison, the CRUST1.0 model (*50*) implies a crust that contains more mass (0.04% of $M_\oplus$) and more moment of inertia of (0.05% of $I_\oplus$) compared to the PREM crust. Reconciling the EPOC mass and moment of inertia with the latest global estimates (*51*) has implications for both the radial distribution of mass,

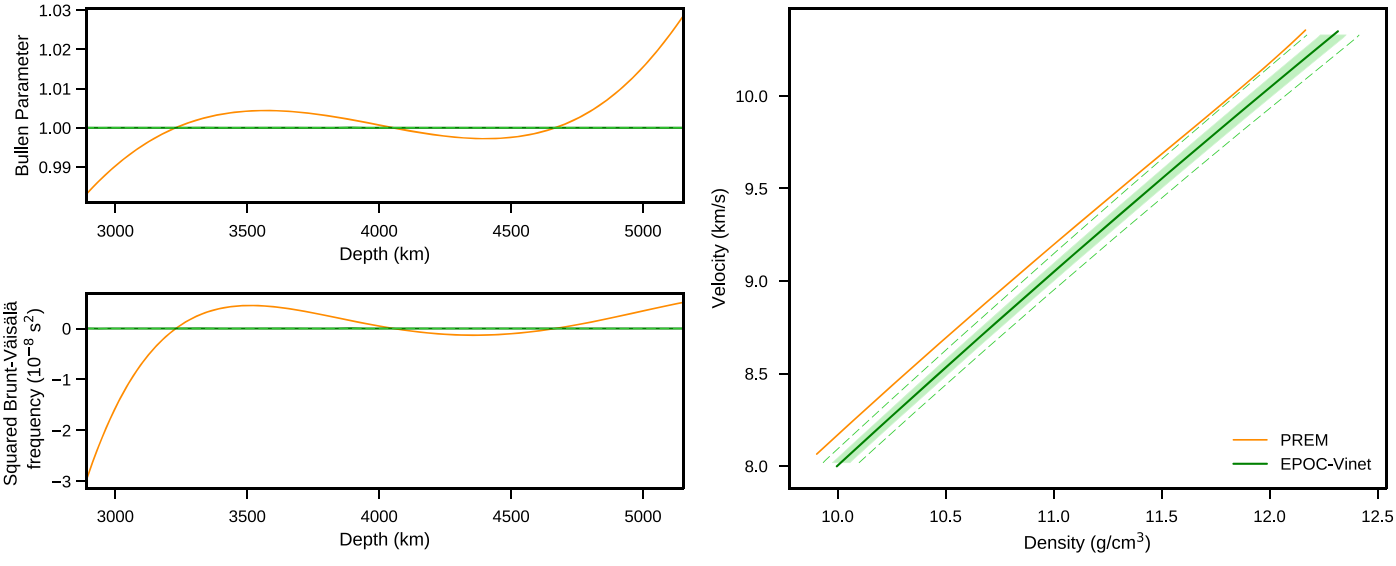

Fig. 4. Relevant physical properties of the EPOC-Vinet and PREM models. Bullen parameter (**top left**) and squared Brunt-Väisälä frequency (**bottom left**) as a function of depth. Velocity as a function of density (**right**). Ranges for velocity and density are calculated when a velocity is predicted by at least 80% of the models. Colors are as in Fig. 2.

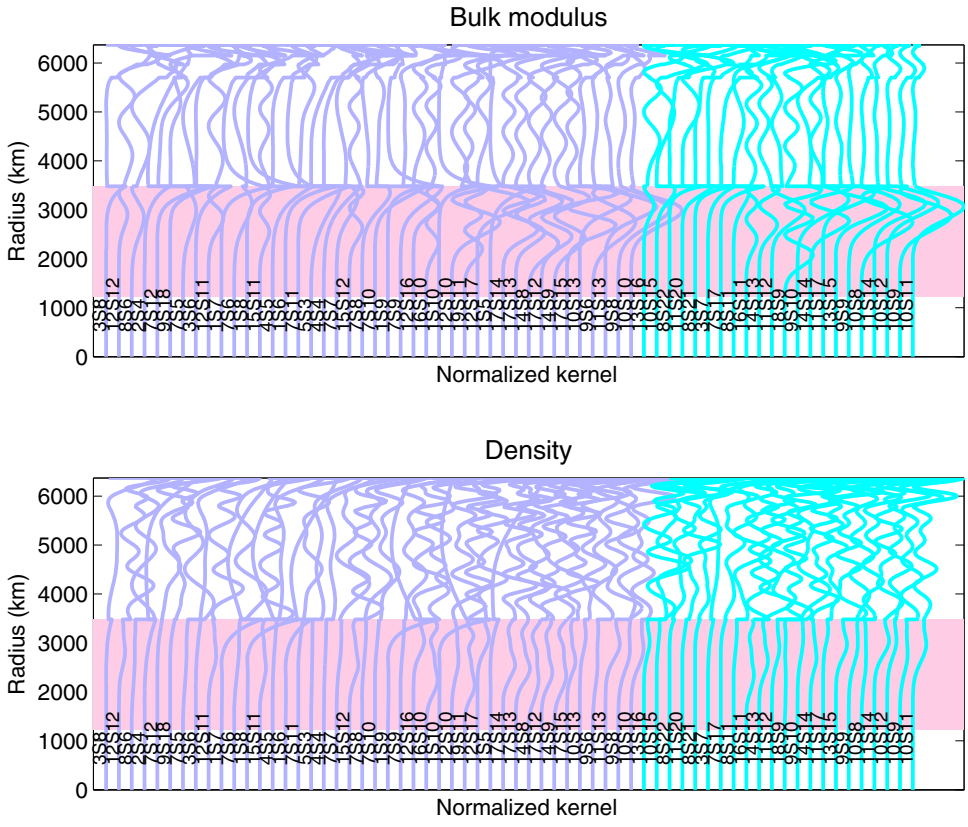

Fig. 5. Mode central frequency sensitivity kernels. Kernels showing sensitivity of mode central frequencies to bulk modulus (top) and density (bottom), for modes that have more than 10% of their sensitivity in the outer core (pink region) for PREM. Modes in teal were not used when PREM was constructed.

including the depths of transition zone discontinuities, and the geographic distribution of density anomalies, such as sinking slabs. The inversion needed to explore these implications is well beyond the scope of this study but should be carried out. Because we do not invert for crust and mantle structure, we do not exclude the alternative explanation that the density of the EPOC core could be an artifact of unexplored tradeoffs with crust and mantle structure beyond those captured by differences between PREM and STW105; the density of the outer core changes when the STW105 is used to describe the rest of Earth (fig. S5).

Counterintuitively, the denser core in EPOC compared to PREM need not imply a reduction in light element content. The EPOC reference molar densities at zero pressures suggest a likely reduction in molar density compared to the best fitting value for PREM. When extrapolating EPOC densities and the Vinet-EoS densities fit to PREM to lower pressures, their densities cross over around 15 GPa. EPOC has steeper gradients in v_p and density across most of the outer core than PREM. Our inverted K_{0S} is lower than that for PREM, while the inverted K'_{0S} is higher than that for PREM, producing the more pronounced decrease in gradient across the outer core compared to PREM. These comparisons suggest that EPOC would be interpreted as a lighter, but more compressible, liquid alloy compared to compositional interpretations based on PREM [for example, (*12*)]. The compressibility of a liquid alloy has been suggested to increase with the presence of different light elements in the outer core (*44*, *49*), so the EPOC model implies a greater fraction of light elements than PREM.

The ICB density increase is not well constrained by our inversion because we do not invert for the density within the inner core; our prior conditions simply require that density does not decrease at the ICB (section S5). Most accepted models suggest that the ICB density increase is smaller than that in PREM; body wave studies have not yet reached a consensus on the density change at the ICB (*52*–*54*).

Using a compilation including recently measured normal mode center frequencies, we have inferred both the mineral physics EoS parameters and the seismological models that best describe the well-mixed liquid iron alloy, which constitutes Earth's outer core. The EPOC model's seismic velocity at the top of the outer core, though derived using normal mode data, is more consistent with previous body wave models than PREM, resolving a long-standing inconsistency between models derived with the two data types. EPOC, combined with PREM to represent the crust and mantle, also fits published differential travel time residuals better than other smooth 1D velocity models of Earth, reducing the need to invoke a thick, anomalously slow layer at the top of the outer core. The EoS parameterization we use also allows the parameters of EPOC to be directly compared with isentropic experimental and computational results, providing information valuable in the endeavor to better understand the composition of Earth's outer core. Furthermore, EPOC's parameters provide a natural EoS to approximate liquid cores of other rocky (exo-)planets.

MATERIALS AND METHODS

Seismic data selection

Our seismic data are normal mode center frequencies. Compared to body waves, which are often used to map structure in the core, mode

center frequencies are less sensitive to lateral heterogeneity in the mantle and crust. Furthermore, whereas body wave travel times can be geographically biased due to the inhomogeneous distribution of earthquakes and stations, normal mode center frequencies effectively homogenize sensitivity across the globe, providing less biased constraints. Finally, unlike body wave travel times, mode center frequencies are sensitive to density. We primarily used the frequencies published in an extensive recent study (*21*), supplemented by data from other sources (*22*–*25*).

To avoid modes that can be strongly affected by lateral variations in structure, we omitted from consideration a number of modes, although they have some sensitivity to the outer core. These fall predominantly into two classes: modes that may couple strongly due to inner core anisotropy (*55*, *56*) and Stoneley modes (*22*). We did not use modes we recognized as inner core–sensitive, excluding those that have more than 0.3% of their κ, μ, or ρ (bulk modulus, shear modulus, or density) sensitivity kernels in the inner core; even modes with very small amounts of sensitivity below the ICB can be affected by inner core structure (*57*, *58*). The Stoneley modes are oscillations confined to the CMB; they are only observed by their cross-coupling interactions with other modes and are also very sensitive to the velocity gradients at the bottom of the mantle, which show significant lateral variation and cannot be represented by a 1D model. A small number of difficult-to-measure modes affected by the Stoneley modes from (*22*) were also not used. With all these factors taken into consideration, we compiled a data set of 319 modes.

Of the modes used, 64 are strongly sensitive to the outer core, with more than 10% of their average κ and ρ sensitivity there; sensitivity kernels for bulk modulus and density for these modes are shown in Fig. 5. The outer core sensitivity was determined by averaging the fractional bulk modulus and ρ sensitivities to the outer core for PREM. This measure does not take into account the relative strength of v_s, v_p, and ρ sensitivity in the rest of Earth; however, these 64 modes show a much better fit when the outer core model is updated from PREM to EPOC, indicating that it is a suitable measure of sensitivity to the outer core. Twenty-two of the strongly outer core–sensitive modes we used were not present in the inversion that produced PREM and the frequencies of modes that were used in the construction of PREM have since been updated by measuring new data.

Published uncertainties for the eigenfrequencies vary widely between studies due to the different approaches adopted for estimating them. Here, we chose to assign uncertainties that acknowledge the potential effects of mantle structure by giving less weight to those modes that are sensitive to replacing the mantle model used. To construct new uncertainties, we computed center frequencies using the 1D reference model STW105 (*27*). STW105 is significantly different in the mantle from PREM, whereas it is virtually identical in the outer core. We assigned each mode's uncertainty to be the larger of the difference between the two frequencies (ranging between 0.01 and 17.9 μHz) and the mean difference across all the modes used (3.2 μHz). Ninety-three percent of our assigned uncertainties are larger than the published uncertainties. We worked using the assumption that the uncertainties were uncorrelated from mode to mode; future work may relax this commonly made assumption. The list of mode center frequencies and errors used is included in section S8.

Parameterization

Vinet's EoS was derived using an approximate energy formulation (*28*) and expressed using three parameters: K_0, the bulk modulus at ambient conditions; K_0', the derivative of the bulk modulus with pressure; and V_0, the molar volume at ambient conditions. While this EoS was derived for the behavior of solids under isothermal conditions (*28*), it can be used to capture the behavior of materials at constant entropy and high pressures (*59*). Here, we inferred the isentropic parameters K_{0S} and K_{0S}', as the temperature across the core and thermal pressure cannot be constrained by our data set, and the outer core is expected to be isentropic. In the Supplementary Materials, we detailed our implementation of, and results obtained using, the third-order Birch-Murnaghan EoS. We found that the velocity and density profiles obtained across the outer core were very similar when using either of these two EoSs.

We used the implementation of the Vinet EoS in BurnMan (*30*). The open source BurnMan code computes seismic properties from a given EoS at specified pressures. The primary assumption, which is important for the purposes of this study, is that the specified EoS (Vinet or Birch-Murnaghan) is appropriate for a liquid metal for the pressure range under consideration. The Vinet EoS formulation was used to solve for volume V at pressure P

$$P = 3K_{0S}\bar{V}^{-\frac{2}{3}}\left(1-\bar{V}^{\frac{1}{3}}\right)\exp\left[\eta\left(1-\bar{V}^{\frac{1}{3}}\right)\right] \quad (2)$$

with

$$\bar{V} = \frac{V}{V_0} \quad (3)$$

$$\eta = \frac{3}{2}(K_{0S}' - 1) \quad (4)$$

Next, the density can be computed, using the molar mass M

$$\rho = \frac{M}{V} \quad (5)$$

We used this density to recompute the pressure inside the outer core. The new pressures were used to recompute new volumes and densities, and we iterated this procedure until the pressures converged. When calculating the pressure throughout our outer core, we used a fixed P (CMB) of 135.75 GPa and a fixed g(ICB) of 4.4002 m/s^2, so the planet as a whole is not self-consistent.

Using the Vinet EoS formulation, molar mass should be another unknown to our problem. However, our data are sensitive to density, that is, molar mass and molar volume trade off perfectly and, effectively, only the molar density can be constrained. To avoid mapping the entire trade-off space, and obtaining unphysical molar mass and volume values in our solution space, we fixed the molar mass at 0.05 kg/mol and inverted for the molar volume. This molar mass is ~10% lower than that of pure iron, which is the correct order of magnitude expected for the outer core (*2*). Here, we presented molar density instead of molar volume, which was not affected by our assumption of molar mass. However, assuming that a fixed molar mass does affect the distribution of molar volumes in our ensemble solution. Molar volume, in turn, trades off with K_{0S} and K_{0S}'; thus, the molar mass assumption does indirectly affect the value of the EPOC EoS parameters.

From the Vinet EoS, we obtained the following formulation for the bulk modulus, K_S

$$K_S = K_{0S}\bar{V}^{-\frac{2}{3}}\left[1+\left(\eta\bar{V}^{\frac{1}{3}}+1\right)\left(1-\bar{V}^{\frac{1}{3}}\right)\right]\exp\left[\eta\left(1-\bar{V}^{\frac{1}{3}}\right)\right] \quad (6)$$

with which we can compute the bulk sound or P wave velocity, v_p

$$v_\mathrm{p} = \frac{K_S}{\rho} \quad (7)$$

SUPPLEMENTARY MATERIALS

Supplementary material for this article is available at http://advances.sciencemag.org/cgi/content/full/4/6/eaar2538/DC1

section S1. Birch-Murnaghan EoS
section S2. EPOC-Birch Murnaghan results
section S3. Inversion using PREM data
section S4. Inversion using STW105 for the rest of Earth
section S5. Previous geophysical tests
section S6. Body wave differential travel time predictions
section S7. Nonlinearity of center frequencies
section S8. Mode data set
section S9. Model values
fig. S1. Parameter posterior distributions and trade-offs for the three Birch Murnaghan EoS parameters.
fig. S2. The EPOC-BM velocity and density models.
fig. S3. Relevant physical properties of the EPOC-Vinet and PREM models.
fig. S4. Models produced by inversion of PREM data.
fig. S5. Models produced using STW105 for the rest of Earth.
fig. S6. Body wave differential travel time predictions.
fig. S7. Nonlinearity of the relationship between mode center frequency and elastic parameters of the core.
table S1. Elastic parameters for the outer core for the Birch-Murnaghan EoS and for Birch-Murnaghan EoS fits to PREM.
table S2. Mode center frequencies used.
table S3. The EPOC-Vinet model and associated velocity and density ranges.
table S4. The EPOC-BM model and associated velocity and density ranges.
References (*61*, *62*)

REFERENCES AND NOTES

1. H. Jeffreys, The rigidity of the Earth's central core. *Mon. Not. R. Astron. Soc. Geophys.* **1**, 371–383 (1926).
2. F. Birch, Elasticity and constitution of the Earth's interior. *J. Geophys. Res.* **57**, 227–286 (1952).
3. D. J. Stevenson, Models of the Earth's core. *Science* **214**, 611–619 (1981).
4. F. Gilbert, A. M. Dziewonski, An application of normal mode theory to the retrieval of structural parameters and source mechanisms from seismic spectra. *Philos. Trans. R. Soc. Lond. A* **278**, 187–269 (1975).
5. A. M. Dziewonski, A. L. Hales, E. R. Lapwood, Parametrically simple Earth models consistent with geophysical data. *Phys. Earth Planet. Inter.* **10**, 12–48 (1975).
6. A. M. Dziewonski, D. Anderson, Preliminary reference Earth model. *Phys. Earth Planet. Inter.* **25**, 297–356 (1981).
7. B. L. N. Kennett, E. R. Engdahl, R. Buland, Constraints on seismic velocities in the Earth from travel times. *Geophys. J. Int.* **122**, 108–124 (1995).
8. A. Morelli, A. M. Dziewonski, Body wave traveltimes and a spherically symmetric *P*- and *S*-wave velocity model. *Geophys. J. Int.* **112**, 178–194 (1993).
9. R. W. L. de Wit, P. J. Käufl, A. P. Valentine, J. Trampert, Bayesian inversion of free oscillations for Earth's radial (an)elastic structure. *Phys. Earth Planet. Inter.* **237**, 1–17 (2014).
10. F. D. Stacey, High pressure equations of state and planetary interiors. *Rep. Prog. Phys.* **68**, 341–383 (2005).
11. J.-P. Poirier, Light elements in the Earth's outer core: A critical review. *Phys. Earth Planet. Inter.* **85**, 319–337 (1994).
12. J. Badro, A. S. Côté, J. P. Brodholt, A seismologically consistent compositional model of Earth's core. *Proc. Natl. Acad. Sci. U.S.A.* **111**, 7542–7545 (2014).
13. D. Alfè, M. J. Gillan, G. D. Price, Composition and temperature of the Earth's core constrained by combining ab initio calculations and seismic data. *Earth Planet. Sci. Lett.* **195**, 91–98 (2002).
14. B. L. N. Kennett, On the density distribution within the Earth. *Geophys. J. Int.* **132**, 374–382 (1998).
15. G. Masters, D. Gubbins, On the resolution of density within the Earth. *Phys. Earth Planet. Inter.* **140**, 159–167 (2003).
16. X. Song, D. V. Helmberger, A *P* wave velocity model of Earth's core. *J. Geophys. Res.* **100**, 9817–9830 (1995).
17. S. Tanaka, Possibility of a low *P*-wave velocity layer in the outermost core from global *SmKS* waveforms. *Earth Planet. Sci. Lett.* **259**, 486–499 (2007).
18. G. Helffrich, S. Kaneshima, Outer-core compositional stratification from observed core wave speed profiles. *Nature* **468**, 807–810 (2010).
19. S. Kaneshima, G. Helffrich, *Vp* structure of the outermost core derived from analysing large-scale array data of *SmKS* waves. *Geophys. J. Int.* **193**, 1537–1555 (2013).
20. S. Kaneshima, Array analyses of SmKS waves and the stratification of Earth's outermost core. *Phys. Earth Planet. Inter.* **276**, 234–246 (2018).
21. A. Deuss, J. Ritsema, H. van Heijst, A new catalogue of normal-mode splitting function measurements up to 10 mHz. *Geophys. J. Int.* **193**, 920–937 (2013).
22. P. Koelemeijer, A. Deuss, J. Ritsema, Observations of core-mantle boundary Stoneley modes. *Geophys. Res. Lett.* **40**, 2557–2561 (2013).
23. T. G. Masters, R. Widmer, *Free Oscillations: Frequencies and Attenuations* (American Geophysical Union, 1995), vol. 1, pp. 104–125.
24. J. S. Resovsky, M. H. Ritzwoller, New and refined constraints on three-dimensional Earth structure from normal modes below 3 mHz. *J. Geophys. Res.* **103**, 783–810 (1998).
25. Reference Earth Model, http://igppweb.ucsd.edu/gabi/rem.html [accessed 3 August 2016].
26. F. A. Dahlen, J. Tromp, *Theoretical Global Seismology* (Princeton Univ. Press, 1998).
27. B. Kustowski, G. Ekström, A. M. Dziewoński, Anisotropic shear-wave velocity structure of the Earth's mantle: A global model. *J. Geophys. Res.* **113**, B06306 (2008).
28. P. Vinet, J. Ferrante, J. H. Rose, J. R. Smith, Compressibility of solids. *J. Geophys. Res.* **92**, 9319–9325 (1987).
29. F. Birch, Finite elastic strain of cubic crystals. *Phys. Rev.* **71**, 809–824 (1947).
30. S. Cottaar, T. Heister, I. Rose, C. Unterborn, BurnMan: A lower mantle mineral physics toolkit. *Geochem. Geophys. Geosyst.* **15**, 1164–1179 (2014).
31. F. Cammarano, A short note on the pressure-depth conversion for geophysical interpretation. *Geophys. Res. Lett.* **40**, 4834–4838 (2013).
32. A. Patil, D. Huard, C. J. Fonnesbeck, PyMC: Bayesian stochastic modelling in Python. *J. Stat. Softw.* **35**, 1–81 (2010).
33. J. H. Woodhouse, The calculation of the eigenfrequencies and eigenfunctions of the free oscillations of the Earth and Sun, in *Seismological Algorithms: Computational Methods and Computer Programs*, D. J. Doornbos, Ed. (Academic Press, 1988), chap. IV.2.
34. G. Masters, M. Barmine, S. Kientz, *Mineos* (California Institute of Technology, 2011).
35. B. L. N. Kennett, E. R. Engdahl, Traveltimes for global earthquake location and phase identification. *Geophys. J. Int.* **105**, 429–465 (1991).
36. J. R. Lister, B. A. Buffett, Stratification of the outer core at the core-mantle boundary. *Phys. Earth Planet. Inter.* **105**, 5–19 (1998).
37. B. Buffett, Geomagnetic fluctuations reveal stable stratification at the top of the Earth's core. *Nature* **507**, 484–487 (2014).
38. D. R. Fearn, D. E. Loper, Compositional convection and stratification of Earth's core. *Nature* **289**, 393–394 (1981).
39. D. Gubbins, C. J. Davies, The stratified layer at the core–mantle boundary caused by barodiffusion of oxygen, sulphur and silicon. *Phys. Earth Planet. Inter.* **215**, 21–28 (2013).
40. B. A. Buffett, C. T. Seagle, Stratification of the top of the core due to chemical interactions with the mantle. *J. Geophys. Res.* **115**, B04407 (2010).
41. T. Nakagawa, On the thermo-chemical origin of the stratified region at the top of the Earth's core. *Phys. Earth Planet. Inter.* **276**, 172–181 (2018).
42. G. Helffrich, S. Kaneshima, Causes and consequences of outer core stratification. *Phys. Earth Planet. Inter.* **223**, 2–7 (2013).
43. M. Landeau, P. Olson, R. Deguen, B. H. Hirsh, Core merging and stratification following giant impact. *Nat. Geosci.* **9**, 786–789 (2016).
44. J. Brodholt, J. Badro, Composition of the low seismic velocity *E'* layer at the top of Earth's core. *Geophys. Res. Lett.* **44**, 8303–8310 (2017).
45. K. Hirose, G. Morard, R. Sinmyo, K. Umemoto, J. Hernlund, G. Helffrich, S. Labrosse, Crystallization of silicon dioxide and compositional evolution of the Earth's core. *Nature* **543**, 99–102 (2017).
46. J. G. O'Rourke, D. J. Stevenson, Powering Earth's dynamo with magnesium precipitation from the core. *Nature* **529**, 387–389 (2016).
47. J. Badro, J. Siebert, F. Nimmo, An early geodynamo driven by exsolution of mantle components from earth's core. *Nature* **536**, 326–328 (2016).
48. F. Birch, Composition of the Earth's mantle. *Geophys. J. Int.* **4**, 295–311 (1961).

49. H. Terasaki, Physical properties of the outer core, in *Deep Earth: Physics and Chemistry of the Lower Mantle and Core*, H. Terasaki, R. A. Fischer, Eds. (Wiley Online Library/American Geophysical Union, 2016), vol. 217, pp. 129–142.
50. G. Laske, G. Masters, Z. Ma, M. Pasyanos, Update on CRUST1.0—A 1-degree global model of Earth's crust. *Geophys. Res. Abstr.* **15**, EGU2013-2658 (2013).
51. F. Chambat, B. Valette, Mean radius, mass, and inertia for reference Earth models. *Phys. Earth Planet. Inter.* **124**, 237–253 (2001).
52. A. Cao, B. Romanowicz, Constraints on density and shear velocity contrasts at the inner core boundary. *Geophys. J. Int.* **157**, 1146–1151 (2004).
53. K. D. Koper, M. Dombrovskaya, Seismic properties of the inner core boundary from PKiKP/P amplitude ratios. *Earth Planet. Sci. Lett.* **237**, 680–694 (2005).
54. H. Tkalčić, B. L. N. Kennett, V. F. Cormier, On the inner-outer core density contrast from PKiKP/PcP amplitude ratios and uncertainties caused by seismic noise. *Geophys. J. Int.* **179**, 425–443 (2009).
55. J. C. E. Irving, A. Deuss, J. Andrews, Wide-band coupling of Earth's normal modes due to anisotropic inner core structure. *Geophys. J. Int.* **174**, 919–929 (2008).
56. J. C. E. Irving, A. Deuss, Stratified anisotropic structure at the top of Earth's inner core: A normal mode study. *Phys. Earth Planet. Inter.* **186**, 59–69 (2011).
57. R. Widmer, G. Masters, F. Gilbert, Observably split multiplets—Data analysis and interpretation in terms of large-scale aspherical structure. *Geophys. J. Int.* **111**, 559–576 (1992).
58. J. Tromp, Support for anisotropy of the Earth's inner core from free oscillations. *Nature* **366**, 678–681 (1993).
59. R. Jeanloz, Shock wave equation of state and finite strain theory. *J. Geophys. Res.* **94**, 5873–5886 (1989).
60. M. Beyreuther, R. Barsch, L. Krischer, T. Megies, Y. Behr, J. Wassermann, ObsPy: A Python toolbox for seismology. *Seismol. Res. Lett.* **81**, 530–533 (2010).
61. H. P. Crotwell, T. J. Owens, J. Ritsema, The TauP Toolkit: Flexible seismic travel-time and ray-path utilities. *Seismol. Res. Lett.* **70**, 154–160 (1999).
62. G. Backus, F. Gilbert, The rotational splitting of the free oscillations of the Earth. *Proc. Natl. Acad. Sci. U.S.A.* **47**, 362–371 (1961).

Acknowledgments: We thank the BurnMan team and, in particular, T. Heister, B. Myhill, I. Rose, and C. Unterborn. We thank S. Chiorini for assistance in data set compilations. We thank A. Shahar, A. Kavner, P. Koelemeijer, S. Merkel, R. Moulik, and Z. Geballe for constructive conversations. Three anonymous reviewers and W. Panero helped us improve this manuscript. **Funding:** J.C.E.I. acknowledges support from the NSF (EAR1644399), and V.L. acknowledges support from the NSF (EAR1345082) and the Packard Foundation. This work started at the 2016 Cooperative Institute for Dynamic Earth Research (CIDER) workshop at the Kavli Institute for Theoretical Physics, University of California, Santa Barbara (supported by the NSF FESD-1135452). **Author contributions:** All the authors participated in the conceptualization, formulation, analysis of the data, modeling, and writing presented in the manuscript. **Competing interests:** The authors declare that they have no competing interests. **Data and materials availability:** All data needed to evaluate the conclusions in the paper are present in the paper and/or the Supplementary Materials. Additional data related to this paper may be requested from the authors.

Submitted 3 November 2017
Accepted 18 May 2018
Published 27 June 2018
10.1126/sciadv.aar2538

Citation: J. C. E. Irving, S. Cottaar, V. Lekić, Seismically determined elastic parameters for Earth's outer core. *Sci. Adv.* **4**, eaar2538 (2018).